

Article

Hydrothermal Carbonization Treatment as a Pathway for Energy Utilization of Municipal Sludge and Agricultural Residues Through Co-Gasification

Georgia Altiparmaki ¹, Dimitrios Liakos ^{1,2}, Andreas Artikopoulos ¹ and Stergios Vakalis ^{1,2,*}

¹ Energy Management Laboratory, Department of Environment, University of the Aegean, University Hill, GR-81100 Mytilene, Greece; envd22004@env.aegean.gr (G.A.); envd23006@env.aegean.gr (D.L.)

² Department of Process Analysis and Plant Design, School of Chemical Engineering, National Technical University of Athens, 9 Iroon Polytechniou, GR-15780 Athens, Greece

* Correspondence: svakalis@chemeng.ntua.gr

Abstract

Municipal sewage sludge (S.S.) and abundant olive-tree pruning on Lesbos Island present both a disposal challenge and an untapped energy resource. This study proposes and evaluates on a preliminary level an integrated system that utilizes both sewage sludge and pruning. The integrated system converts sewage sludge into Hydrochar (HC) via Hydrothermal Carbonization (HTC), removes the aqueous phase using passive solar distillation, and co-gasifies the dried HC with olive pruning in an autothermal downdraft gasifier. HTC experiments on anaerobically digested sludge produced HC with higher heating values exceeding 20 MJ kg⁻¹ while reducing the chemical oxygen demand of the process liquor. Gasification modelling, using the MAGSY equilibrium model, demonstrated that replacing up to 50% of lignocellulosic biomass with HC increased hydrogen content and the Lower Heating Value (LHV) of syngas. Mass and energy balances suggest that the system could provide approximately 590 kW of continuous power, contributing around 4720 MWh to the island's annual electricity generation. These results indicate that combining HTC, solar distillation, and co-gasification offers a viable pathway to close waste loops, reduce landfill needs, and deliver renewable energy. Future work will focus on Aspen Plus design and optimization, along with a life-cycle assessment in order to assess the environmental benefits.

Keywords: hydrothermal carbonization; solar distillation; co-gasification; agrowaste; waste valorization; renewable energy; ecological benefit



Academic Editors: Carmen Branca and Antonio Galgano

Received: 20 July 2025

Revised: 18 August 2025

Accepted: 22 August 2025

Published: 26 August 2025

Citation: Altiparmaki, G.; Liakos, D.; Artikopoulos, A.; Vakalis, S.

Hydrothermal Carbonization

Treatment as a Pathway for Energy Utilization of Municipal Sludge and Agricultural Residues Through Co-Gasification. *Processes* **2025**, *13*, 2713. <https://doi.org/10.3390/pr13092713>

Copyright: © 2025 by the authors. Licensee MDPI, Basel, Switzerland. This article is an open access article distributed under the terms and conditions of the Creative Commons Attribution (CC BY) license (<https://creativecommons.org/licenses/by/4.0/>).

1. Introduction

Three percent (3%) of the total human activity emissions comes from greenhouse gases (GHGs) emitted by wastewater treatment plants (WWTPs) [1]. WWTPs contribute to a reduction in the pollution load of sewage sludge (S.S.), while treated sludge can be reused and valorized for soil amendment or utilized as a biomass feedstock in thermochemical conversion processes for higher energy value materials like HC and syngas [2]. The management of municipal S.S. faces significant challenges, since it serves as an unavoidable contributor to environmental pollution [3]. According to Zhenggang et al. [4], S.S., if deposited in a covered dumping site, not only consumes a significant volume of soil storage but also poses a risk of releasing heavy metals, leading to environmental pollution. Certain heavy metals such as nickel, lead, zinc, cadmium, chromium, copper, and mercury have

the potential to gather in soil and the food chain, posing risks to both plant life and overall human and environmental health due to their phytotoxic effects [5]. Moreover, apart from heavy metals, Urbaniak et al. [6], reported that S.S. has the capacity to accumulate substantial quantities of unregulated substances, like pharmaceuticals, which demonstrate greater stability compared to those present in the initial wastewater. Specifically, antibiotics, constituting substances that favor fats and resist water, have the tendency to attach to activated sludge and are not completely removed during anaerobic digestion, showing a low efficiency in elimination [7]. Achkir et al. [5] mentioned that utilizing treated sludge on land could boost agricultural sustainability by reintroducing nutrients to the soil, aiding plant growth. The global focus on repurposing sludge in agriculture is not solely prompted by disposal issues but also by rising water demand for farming and the scarcity of fresh water worldwide.

S.S. constitutes a mixture of organic, inorganic compounds, pathogenic microorganisms, and other microbiological pollutants [8]. It is also worth mentioning that S.S.s have 1 to 4% *w/w* solids and high moisture content [9]. According to Xu et al. [10], the need for S.S. treatment has attracted a lot of interest globally due to the environmental pollution that sludge can cause. One of the most common methods utilized for sludge treatment is Anaerobic Digestion (AD) and numerous studies have been published on this topic [11]. Due to the high moisture content of S.S, another appropriate technology for the treatment of wet organic solid waste like this is HTC [10], which also has the advantage of being a thermal technology. According to Pérez et al. [12], the HTC process is one of the most studied Waste-to-Energy technologies. The Hydrothermal Treatment (HT) process propagates with the presence of subcritical conditions of water, i.e., increased temperatures and pressure [13]. In more detail, HTC constitutes a thermochemical process with exothermal reactions that can be appropriate for the conversion of S.S. into a carbonaceous product which is called HC. [14]. The temperature, pressure, and residence time rates where the HTC process take place are between 180 and 280 °C, 10 to 80 bar and from some minutes to several hours, respectively, according to Maniscalco et al. [15]. In addition to this, Maniscalco et al. [15] mentioned that HC has high energy content and an ecological character that make this product suitable for many environmental applications.

Biomass is a low carbon energy source which can be used as feedstock for a number of valuable products including fuels and chemicals. Gasification is a process in which high percentages of the biomass input are converted to an energy-rich gaseous fuel, usually referred to as syngas or producer gas [16]. According to Nunes [17], syngas is a mixture of hydrogen, nitrogen, methane, carbon monoxide, and carbon dioxide. The applications of syngas include its utilization for electricity generation, and the production of chemicals and biofuels. The gasification process takes place at temperatures between 800 and 1000 °C [18]. Srimalanon et al. [19] highlighted that the gasification systems can effectively remove toxic elements in solid waste. The co-gasification of biomass with other fuels offers several advantages, e.g., enhancing the reactivity of the fuel mixture and improving the overall efficiency of the gasification process. Recent studies reported that increasing the proportions of biomass in the input mix and elevated temperatures enhance the gasification reactivity of char. A significant synergistic effect on co-gasification reactivity was observed at 1000 °C, but this effect gradually weakens with further temperature increases from 1000 °C to 1100 °C [20–22].

Rising energy needs from industrialization and economic growth strain fossil fuel resources, increasing CO₂ emissions and global warming. Researchers are pursuing sustainable alternatives like hydrogen and biomass to reduce these impacts. Notably, HTC converts biomass into HC, which serves as fuel or a biofuel precursor [20]. A recent study by Fona et al. [23] indicated that an efficient catalyst is important for effective gasification.

The research suggests that the HC produced from the HTC process can function as a catalyst during gasification, which may improve syngas production. Other recent studies have delved into the co-gasification of HC with various fuels, aiming to augment energy recovery and enhance fuel quality [24]. This method, which produces syngas—a hydrogen and carbon monoxide blend—by co-gasifying HC with coal, biomass, or municipal solid waste, presents numerous advantages [20]. These include efficient utilization of diverse feedstocks, improved fuel quality by minimizing water content and chlorine, and increased energy density. Moreover, co-gasification synergistically leverages the distinct properties of combined fuels to enhance energy recovery. The resultant hydrogen-rich syngas serves as a clean energy source for power generation or as a chemical production feedstock, thus diminishing fossil fuel dependence and aiding greenhouse gas emission reduction. Additionally, this approach offers a solution to the tar formation challenge often encountered in biomass gasification. By separating biomass pyrolysis and char gasification stages, it enables effective tar management, thereby enhancing the gasification process's efficiency and cleanliness [23]. In summary, HC co-gasification stands out as a promising strategy for optimizing energy recovery, refining fuel quality, and addressing environmental concerns associated with conventional fuels.

This study explores the application of HTC to transform municipal sludge into HC and a hydrothermal liquid using a small-scale HTC reactor that is presented in Section 2. Downstream, the process involves the separation of the liquid fraction through solar distillation, using a solar still to dry the solid product and recover the water from it with exclusive solar energy, thus offering both economic and energy benefits. This system was constructed and operates in the Energy Management Laboratory of the University of the Aegean. Furthermore, the present research examines the feasibility of combined gasification of the resulting hydrocarbon with agricultural biomass residues, mainly from olive tree pruning. The developed model is also presented in the next section. The innovation of this study is the combination of all three technologies for the first time with the aim of sustainable waste management and energy production by evaluating their practicality and efficiency. The framework of the balance analysis is presented in the following section and takes into account the utilization of the available sewage sludge and pruning of the island of Lesvos.

2. Materials and Methods

2.1. Materials

Samples of S.S. were collected from the WWTP of Mytilene (Lesvos, Greece) and anaerobically digested sludge (A.D.S.) was collected from Antissa (Greece), a village on Lesvos Island, Greece, within the framework of the Hydrousa project.

2.2. Design of Experiments and Reactors Design

Two series of six experiments of HTC took place in this study. In the first sequence, all the HTC experiments were conducted with A.D.S. while in the second all the experiments were conducted with S.S. The first three experiments of the first sequence took place in a PTFE 25 mL hydrothermal reactor filled with 7.5 gr, 10 gr, and 12.5 gr of A.D.S. per experiment, under 24 h residence times and autogenous pressures at 200 °C temperature rates inside an oven. The next three experiments took place under the same conditions with the only difference being in temperature, which was 220 °C. The six final experiments of the second sequence took place exactly as the first sequence but with S.S. After each experiment and before the sample collection, the reactor was placed in a water bath at room temperature to stop further thermochemical reactions until it reached room temperature conditions. Both the selection of the reactor fillings and the experimental conditions chosen,

such as temperature and residence times, were based on a previous study by Vasileiadou et al. [25]. Table 1 below presents the operation conditions of each experiment in detail and Figure 1 the hydrothermal reactor that was utilized for the experiments.

Table 1. Experimental conditions.

Experiment	Reactor Material/Filing (gr)	Temperature (°C)	Pressure	Residence Time (hours)
HC-1	Anaerobic sludge/7.5 gr	200	Autogenous pressure	24
HC-2	Anaerobic sludge/10 gr	200	Autogenous pressure	24
HC-3	Anaerobic sludge/12.5 gr	200	Autogenous pressure	24
HC-4	Anaerobic sludge/7.5 gr	220	Autogenous pressure	24
HC-5	Anaerobic sludge/10 gr	220	Autogenous pressure	24
HC-6	Anaerobic sludge/12.5 gr	220	Autogenous pressure	24
HC-7	Sewage sludge/7.5 gr	200	Autogenous pressure	24
HC-8	Sewage sludge/10 gr	200	Autogenous pressure	24
HC-9	Sewage sludge/12.5 gr	200	Autogenous pressure	24
HC-10	Sewage sludge/7.5 gr	220	Autogenous pressure	24
HC-11	Sewage sludge/10 gr	220	Autogenous pressure	24
HC-12	Sewage sludge/12.5 gr	220	Autogenous pressure	24



Figure 1. 25 mL PTFE Hydrothermal reactor.

2.3. SOLAR Distillation

The study of Mastoras et al. [26] mentioned that, due to solar distillation, water recovery is simultaneously achieved through the process of natural evaporation with energy supplied exclusively by the sun and also resulting in the moisture removal of wastewater and sludges. Referring to a study of Leghari et al. [27], HC of the S.S. was utilized for syngas production through a gasification process, which was subjected to

conventional oven drying at 105 °C for 24 h. In this case, the integration of a solar still in the system has the advantage that through solar distillation not only the drying of the hydrocarbon produced by HTC can be effectively carried out before its utilization for gasification without the use of conventional and costly drying methods in terms of economy and energy, but also for water recovery that gives the system a strong cyclic character.

This energy usage is relatively modest, indicative of an application that balances energy expenditure with the functional demands of temperature maintenance. The reported evaporation rate of approximately 4 L per day for every square meter (L/d m²) illustrates a significant water loss, a consequence of the sustained high temperatures. Such a rate necessitates a diligent approach to fluid management, ensuring that the system's hydration is maintained to prevent operational interruptions or damage. With a total area of 2.5 square meters, the system's footprint is compact, suggesting a design that prioritizes space efficiency. This size is adequate for its intended purpose, which is to support the continuous operation of the 4570A Parr hydrothermal reactor. The reactor, which operates under conditions of elevated temperature and pressure, is typically utilized in chemical research and industrial applications for synthesizing materials and chemicals that require such extreme conditions.

In summary, the system presents a specialized setup configured to meet the rigorous demands of hydrothermal reactions. Through its heated floor and efficient pump system, it maintains a stable high-temperature environment conducive to the operations of the Parr hydrothermal reactor. Despite the challenges posed by water evaporation, the system's design reflects a careful consideration of energy efficiency and spatial economy, ensuring its viability for continuous industrial or research applications [23].

Figure 2 illustrates an integrated concept that synergizes HTC, solar distillation, and the co-gasification of HC with wood chips. A key advantage of this integrated system is the use of solar distillation, which effectively bypasses the need for energy-intensive drying methods traditionally required to remove water from the produced HC. This approach not only enhances the energy efficiency of the process but also aligns with sustainable practices by leveraging renewable energy sources.

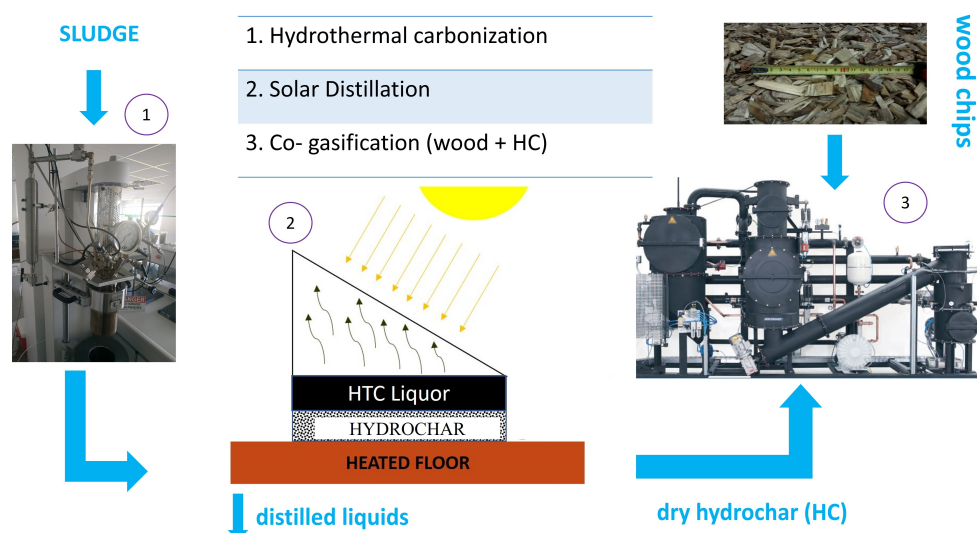


Figure 2. The integrated idea of combining HTC, solar distillation, and co-gasification of HC with wood chips.

2.4. Materials Analysis

For the analysis of the liquid products, pH, Electrical Conductivity, and Chemical Oxygen Demand (COD) measurements were performed. pH and Electrical Conductivity

measurements were conducted with a CONSORT C932 pH—meter and a LF95 Conductivity meter. The COD was determined using a method of Standard Methods for the Examination of Water and Wastewater in which 2.8 mL of silver sulphate, 1.2 mL of potassium dichromate, and 2 mL filtered sample were added, respectively [28]. Additionally, for the preparation of the blank sample, the same sequence was performed instead of the sample in which 2 mL of distilled water was added. The digestion took place in a COD reactor for 2 h and after this procedure the vials cooled to reach room temperature conditions. The last step included the COD measurements with the use of a HACH DR/2400 spectrophotometer. All COD, pH, and Electrical Conductivity measurements operated in triplets.

Moreover, analysis of the solid products, mass yields, and High Heating Value (HHV) measurements were performed. The mass yields were determined by weighing the mass both before and after the experimental procedure. All the samples were dried at 105 °C for 24 h and weighed on a digital analytical balance lab precision scale after reaching room temperature conditions. Heat of Combustion measurements were performed in a Parr 6400 Calorimeter where each one of the dried char samples was burned in the presence of oxygen with the use of a wick in a bomb inside the calorimeter at 29 °C. All Heat of Combustion measurements operated in triplets. Table 2 below presents the analyses carried out on the liquid and solid samples. The statistical analysis of the samples was performed in accordance with the study by Mastoras et al. [26].

Table 2. Analyses of the liquid and solid HTC products.

	Liquid Samples	Solid Samples
Analyses	COD	Mass yield
	pH	HHV
	Conductivity	

2.5. Model and Energy Balances

In this research, the MAGSY model was employed to simulate the gasification of biomass in a downdraft gasifier, as presented by Vakalis and Moustakas [29]. At the heart of the model lies its operation within MATLAB/Cantera, utilizing the sophisticated Villars–Cruise–Smith (VCS) algorithm. This algorithm, primarily designed for solving non-linear optimization problems, is adapted here to minimize chemical potential, yet it encounters certain limitations due to its inherent assumptions, particularly in the context of Gibbs free energy minimization. A pivotal aspect of the model’s efficiency is its reliance on the GRI-Mech mechanism, which, while optimized for methane combustion, has limitations when applied to gasification processes. The model operates under the assumption of ideal gases, a factor that might introduce complexities in pressurized environments, although this is less of a concern in small-scale reactors operating at atmospheric pressure. Additionally, the approximation of char properties, based on the graphite mechanism, does not fully encapsulate the quasi-catalytic effects of char. This points to a fundamental constraint of thermodynamic equilibrium models that inherently assume a state of equilibrium, which may not always reflect real-world conditions, especially in the context of small-scale, fixed-bed reactors where adaptability and computational efficiency are paramount. Moreover, Nunes [17] mentioned in one of his studies that the equilibrium models overpredict the conversion of H₂ and also the delivery of each compound in the gas, under the limitations of the thermodynamics and mass transferring.

As referenced by Vasileiadou et al. [25], Lesvos Island, which is home to approximately 11 million olive trees, faces challenges in the effective management of agricultural biowaste,

especially from olive tree pruning. Lesvos Island has 40,000 t/y of olive pruning that can be available, while the WWTPs of the island also produce 2 kt of municipal sludge annually. Furthermore, the sustainable treatment of municipal sludge remains an unresolved issue in several regions of Greece, including the North Aegean.

2.6. Energy Demand and Production

The values for the energy demand of HTC have been retrieved from the study by Mendecka et al. [30], where the authors provided upper values of 0.03 kWh and 2.3 kWh of energy demand per kg of feedstock, values that are consistent with the literature, as the authors stated. In this framework, we assumed a value of 2.5 kWh per kg of feedstock in order not to underestimate the energy demand and in order to account for this proposed concept that is—by no means—optimized in this study. Weather data for the solar still study were collected every 2 min using a Campbell Scientific (Logan, UT, USA) CR1000 data logger. Ambient temperature was measured with a YOUNG RM (Traverse City, MI, USA) Model 41003-90 Multi-Plate Radiation Shield, while T-type thermocouples tracked air and OMWW temperatures in the still. Solar radiation was monitored by a Kipp & Zonen CMP3 Pyranometer (285–2800 nm, 7–14 $\mu\text{V}/\text{W}/\text{m}^2$ sensitivity), suitable for high irradiance environments. In this study, we also integrate the experimental values for the energy demand of the solar still operation, as they were measured with the presented system by Mastoras et al. [26]. The authors presented an annual consumption of 657 kWh and again in order to provide a realistic number we assumed a value of 700 kWh. The system operates in a controlled environment with average temperatures of 50–55 °C, higher than typical ambient levels but below water's boiling point. It uses a radiant heated floor, distributing heat efficiently via a liquid medium circulated by pumps. These pumps, essential for heat transfer, consume 650–700 kWh of electricity per year. The energy demand data for the modelled autothermal gasifier was extracted for the study by Patuzzi et al. [31], where the authors report (among numerous downdraft gasification technologies) production of more than 1 MWh for every ton of input biomass. In our case, we assumed the production of 1 MWh for every ton of input biomass.

2.7. Limitations of the Study

This study has primarily the scope to introduce the concept and the feasibility of coupling HTC with gasification, and it should be treated as such. Several limitations follow from that scope. The gasification step was analyzed with an equilibrium framework, and only one HC condition (HC4) was advanced to detailed syngas evaluation. At this point we should emphasize that the co-gasification modelling of biomass and HC is a rather novel concept with very few applications. Future work will test multiple HC and ratios by also integrating experimental gasification data that the authors will develop. The energy demand for the utilized reactors and instruments was retrieved by other studies, as mentioned in the previous sections. Future experiments will measure the energy demand by means of energy meters for the case of the HTC reactor, the solar still, and the gasifier. Environmental considerations and scale-up aspects were not quantified: potential emissions, by-product handling, and economic feasibility will be assessed in upcoming studies. These limitations are intrinsic to the scope of this particular study, i.e., to propose and preliminarily validate the HTC–gasification coupling and provide a solid basis for future work.

3. Results and Discussion

Table 3 below presents the composition elements of olive pruning, sludge and HC feedstocks. In a study of Alipour et al. [32], the HC produced from HTC of sludge at

180 °C characterized from 38.02% C, 4.73% H, 15.95% O, 4.46% N, and 35.99% ash content regarding the results presented in this study.

Table 3. Elemental composition of the utilized feedstock.

	Olive Pruning	Sludge	Hydrochar HC-4	Olive Pruning	Sludge	100% HC	20% HC	50% HC
C	48.50	34.9	32.45	C	1.00	1.00	1.00	1.00
H	5.30	4.67	3.11	H	1.31	1.61	1.15	1.22
O	44.70	20.15	11.73	O	0.69	0.43	0.27	0.59
N	0.70	4.38	3.26	N	0.01	0.11	0.09	0.03
Ash	0.80	35.9	49.45					

3.1. Chemical Oxygen Demands Characterization of the Liquid Samples

Figure 3 presents both the COD of the raw sludge before each hydrothermal processing, and the hydrothermal products. In all experiments, COD concentrations increased to a significant extent after the hydrothermal treatment. Similar results were reported also by a recent study of Petrovic et al. [33], where according to measurements COD is estimated around 20 to 100 g/L in the hydrothermally treated samples as well as the treated samples of this study. Moreover, through HTC processing C binding is taking place during the formation of the HC [34], justifying the initial increase in COD values in the experiments conducted at 200 °C (HC-1, HC-2, HC-3) with the subsequent decrease in those performed at 220 °C (HC-4, HC-5, HC-6) as well as the same sequence also observed in the samples HC-7 to HC-9. Similar results were also noticed by a study of Kossinska et al. [35] where under 250 °C (30–120 min), COD decreased compared to the values recorded under operating conditions of 200 °C 30 min. Additionally, Marin-Batista et al. [36] presented a similar sequence of COD rates that highlighted an increase in the concentrations from 180 °C to 210 °C and a decrease from 210 °C to 250 °C suggesting that the decrease at higher temperatures is related to the successive degradation of proteins and some carbohydrates such as cellulose [36]. Another explanation for the decrease in the COD by increasing the operation temperatures was presented in a recent study of Oliveira et al. [37], supporting the theory that the gasification process turns faster than the hydrolysis reactions and the organic substances dissolution that occur over 200 °C. In Table 4, all the COD measurements of the HTC samples are presented in more detail.

Table 4. COD measurements of the HTC samples.

Experiment	COD (mg/L) of HC
Raw A.D.S.	477.8
HC-1	25,130.3
HC-2	25,144.8
HC-3	23,334.6
HC-4	34,332.8
HC-5	22,667.2
HC-6	23,195.8
Raw S.S.	2175.4

Table 4. Cont.

Experiment	COD (mg/L) of HC
HC-7	16,931.8
HC-8	16,374.2
HC-9	15,434.8
HC-10	14,701.4
HC-11	11,991.6
HC-12	13,269.0

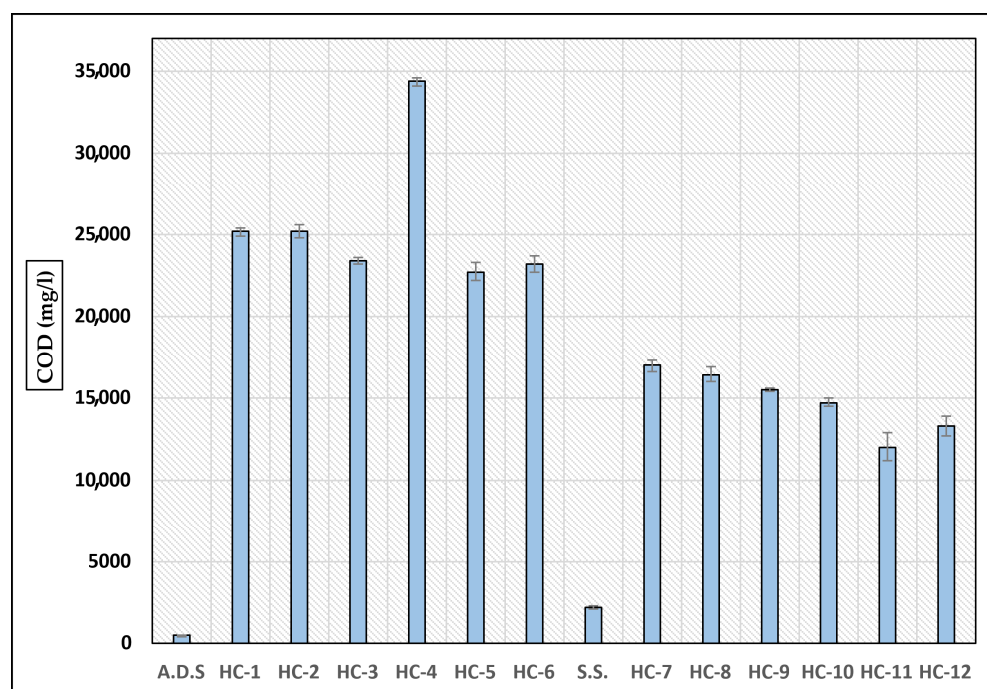


Figure 3. COD measurements of the raw material and hydrothermal products.

3.2. Characterization of Solid Products (HC)

Figure 4 shows the percentage of the HC yield of each experiment. The mass balances of the HC ranged between 40% and 50% while the most satisfactory percentage (50%) was recorded in the experiment that operated under 220 °C and 12.5g reactor filing (HC-6) while 40% occurred in the experiment of 200 °C and 7.5g reactor filing (HC-7). In more detail, the experiments of 10 g and 12.5 g reactor filings at 200 °C recorded higher percentages of HC outputs compared to the corresponding experiments carried out at 220 °C. According to the results of a study by Salimbeni and Demey [38], it was found that by increasing the operating temperature, the amount of the produced gas also increased, while there were no significant differences in solid yield between the experiments performed at 180 °C and at higher temperatures. Moreover, another study of Shrestha et al. [39] mentioned that by increasing the operating temperature in HTC processing, higher biomass decomposition occurs, resulting in low HC yield according to their results. Similar results were also observed in a study of Selvaraj et al. [40], where there was noticed a 13.7% drop of the HC yield from HTC of 180 °C to 300 °C operation temperatures. In addition to this, a 68.32% HC yield under 180 °C of HTC of sludges was noticed in a recent study of Alipour et al. [32], confirming the previous assumption that increasing the operation temperature results in a drop in the HC yield. This pattern is also revealed in our results presented in Figure 4. Other similar results were also reported in a recent study of Duan

et al. [41], where a 54.72% HC yield measured under 190 °C/120 min residence time, 49.96% HC yield at 220 °C/150 min, and 44.04% HC yield/120 min. The explanation for this lies in the hydrothermal reactions that occurred and increased the C content while removing the O, respectively enhancing condensation reactions [42]. Moreover, the elevation of operation temperatures and residence times creates the appropriate conditions for hydrolysis reactions to occur, thus resulting in the presence of more soluble dissolved carbon in the aqueous fraction.

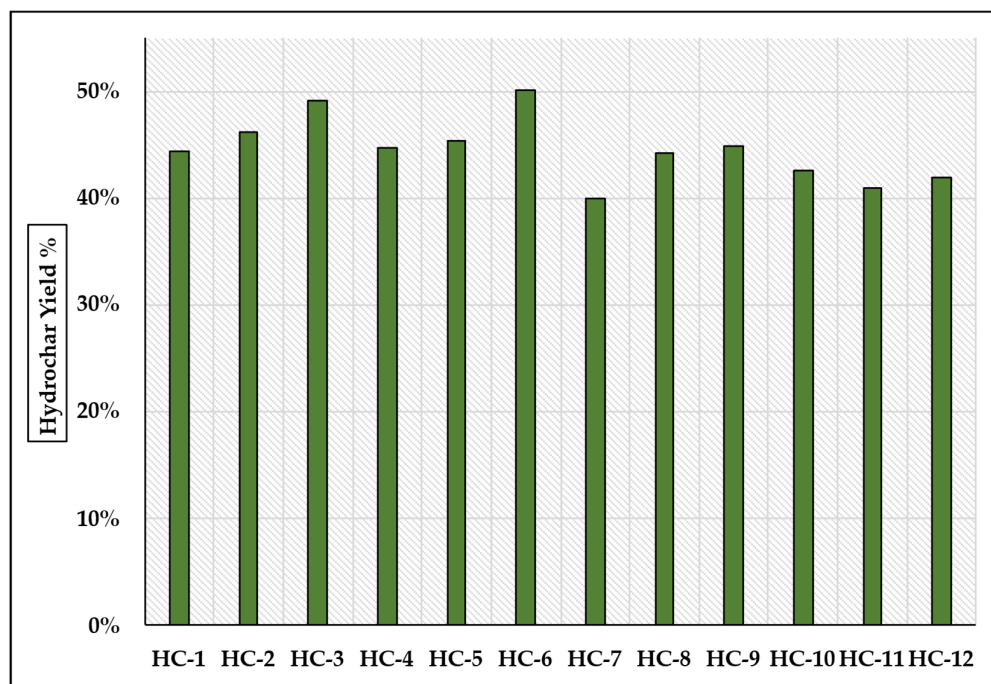


Figure 4. Percentage yield of the produced HC.

3.3. Higher Heating Value of the HC

Figure 5 presents the Higher Heating Value (HHV) of the produced HC of each experiment. The HC produced at 220 °C seemed to have a HHV than those produced at 200 °C, especially (HC-10) that observed the maximum HHV range 37.37 MJ/kg. Similar results are presented in a study of Zhi et al. [42] where the researchers noticed that the HHV of HC produced from 180 °C to 240 °C ranged between 10.4 and 11.57 MJ/kg. In addition to this, they also mentioned that HTCs around 200 to 250 °C and 180 to 300 min are ideal reaction conditions for enhancing the HHV of the HC. Other similar results were presented by a recent study of Duan et al. [41] where the HHV of the HC produced under 190 °C was 12.67 MJ/kg and at 220 °C was 11.19 MJ/kg respectively. According to the results of a study by Gong et al. [43], it was found that by increasing the proportion of biomass, the HHV enhances, but this also depends on the feedstock type. Moreover, the selected operating temperature can determine the calorific value as mentioned in a study of Vasileiadou et al. [25]. In a study of Mazumder et al. [44], the coal from sludge treated by HTC showed energy values of 3.86 MJ/kg at 190 °C, increasing to 4.67 MJ/kg at 210 °C and 5 MJ/kg at 230 °C, likely due to fixed carbon produced during devolatilization. However, they noted that other studies reported higher calorific value values in their results due to higher carbon content in the sludge [44]. Table 5 below shows the HHV of the produced HC in more detail.

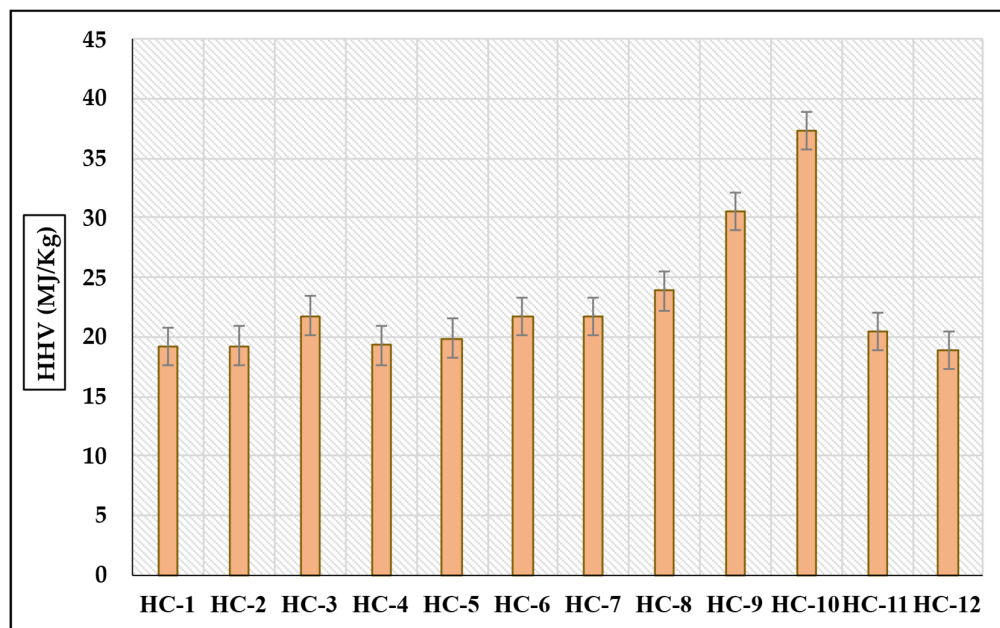


Figure 5. HHV measurements of the produced HC.

Table 5. HHV of the produced HC.

Experiment	HHV (MJ/kg)
HC-1	19.16
HC-2	19.27
HC-3	21.77
HC-4	19.29
HC-5	19.88
HC-6	21.74
HC-7	21.69
HC-8	23.87
HC-9	30.53
HC-10	37.37
HC-11	20.48
HC-12	18.86

3.4. LHV of the HC and % Molar Fraction of the Produced Gases

A bar chart in Figure 6 illustrates the molar fraction percentages of different gases and the LHV produced from various feedstocks: Olive pruning, HC (HC-4), 20% HC, and 50% HC. In the chart, the blue bars represent the molar fraction of carbon monoxide (CO); The orange bars represent the molar fraction of carbon dioxide (CO₂); The yellow bars indicate the molar fraction of hydrogen (H₂); The grey line tracks the LHV in MJ/kg.

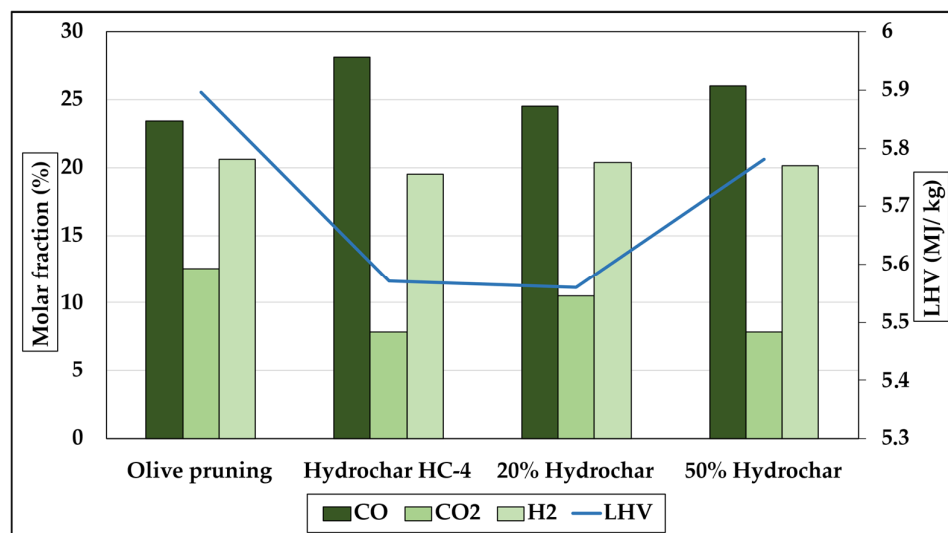


Figure 6. Molar fraction % of different gases and the LHV produced from olive pruning, Hydrochar HC-4, 20% HC, and 50% HC.

From olive pruning to 50% HC, we can observe changes in the composition of the gases and the energy content of the output. It seems that as the percentage of HC increases, the molar fraction of hydrogen also increases, which is typically desirable in gasification processes for energy production due to hydrogen's high energy content. According to a study of Leghari et al. [27], the increase in H₂ and CO depends on the depolymerization of organic molecules as well as the thermal cracking that enhances the syngas production and decreases the transformation to CO₂ and H₂O. In a recent study of Chen et al. [45], two heating values of H₂ were reported as 11.70 MJ/Nm³ (HHV) and 6.24 MJ/Nm³ (LHV) under 1449.85 °C to 1749.85 °C adiabatic flame temperatures. The component volumetric fractions of the gases were 21% H₂, 23% CO, 3% CH₄, 10% CO₂, and 43% N₂, respectively. Additionally, there is a variation in the LHV among the different feedstocks. The LHV appears to be highest for the 50% HC mix, which correlates with the increased presence of hydrogen, a high-energy gas. This data could be used to evaluate the efficiency and energy potential of different feedstock mixtures in a gasification process, allowing for optimization of the process towards the most energy-rich and sustainable output.

Figure 7 presents the pH and conductivity measurements of the HTC liquid samples. According to this, it seems that both the pH and conductivity were influenced by the elevated temperature from 200 °C to 220 °C. In lower temperatures, the concentrations of organic acids and amino acids in the liquids are higher and this lowers the pH rates [27,35]. Moreover, the different conductivity rates show the complexity of the reactions that occur through the HTC process.

3.5. Energy Output of the Integrated System

Figure 7 presents the preliminary analysis of the flows for the integrated process. It consists of HTC, passive solar drying, and gasification technologies. This process exemplifies an integrated approach to waste management and energy recovery, contributing significantly to the circular economy. The process initiates with the input of sludge, approximately 2000 tonnes annually, into the HTC system. HTC is a thermochemical process that transforms organic materials into a coal-like substance known as HC. This stage alone is responsible for generating about 180 MWh of energy per year. The outputs of the HTC process are multifaceted. It yields HTC products, such as HC, at a substantial rate of 1600 tonnes per year. Additionally, the process produces HTC gases, amounting to 400 tonnes annually, which hold potential for energy generation or further chemical

processing. Another significant output is HTC liquors, totalling 880 tonnes per year. These are water-based solutions containing various chemicals, offering possibilities for recycling or use as feedstock in other processes.

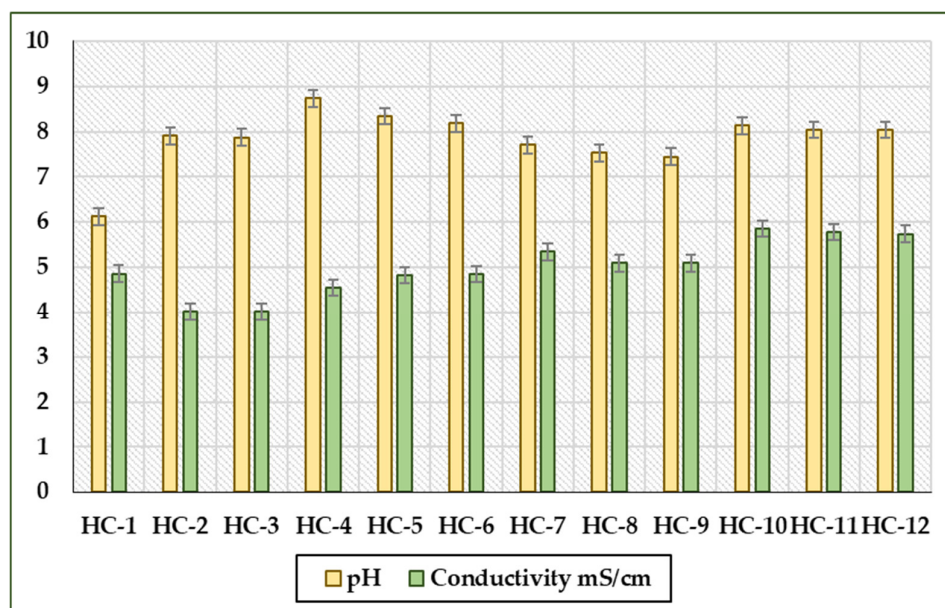


Figure 7. pH and conductivity values of the HTC liquid samples.

In a parallel stream, the system processes olive pruning biomass, amounting to 4000 tonnes per year, through gasification. This technology converts carbonaceous materials into a synthesis gas comprising carbon monoxide, hydrogen, and carbon dioxide by reacting with the material at elevated temperatures with controlled oxygen and/or steam. The energy yield from this stage is impressive, with an output of 4720 MWh per year. The HC produced, quantified at 720 tonnes per year, undergoes a recovery process, although the specifics of this stage are not detailed in the image. Additionally, the system incorporates a solar still, contributing 700 kWh of energy annually. Solar stills typically operate by using solar energy to evaporate water, effectively separating it from salts and impurities, and then condensing the purified water. The energy outputs from the gasification process are significant, featuring a continuous power output of 590 kW and a total annual energy production of 4539 MWh. Overall, the diagram in Figure 8 represents a sophisticated and environmentally conscious process that effectively turns waste materials like sludge and olive pruning into valuable energy and products. This system not only addresses waste management challenges but also contributes to energy generation, highlighting a sustainable and innovative approach in the field of renewable energy and resource management.

3.6. Economic Assessment

According to a study of Saba et al. [46], the cost of HTC is higher than the heating value that this process can produce in comparison with other commercially available options. However, HTC constitutes a profitable process due to the combined value cost of the byproducts. Providing some financial data, the HC of sludge has a selling price estimated about USD 169/ton HC while olive pruning has one of USD 150/ton HC [33]. As for the solar distillation operation cost, it is estimated to be about EUR 0.6/m³ while the total cost was determined around EUR 1.21/m³ according to a study of Mastoras et al. [26].

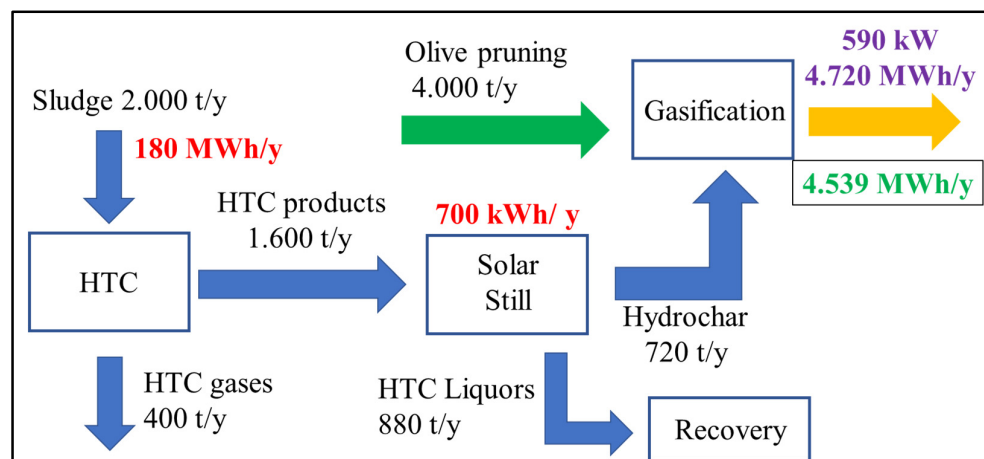


Figure 8. A completed system that effectively turns waste materials like sludge and olive pruning into valuable energy and products.

3.7. Limitations of the Study Results and Future Work

The present work is necessarily exploratory by assessing the “gas phase” behavior from the MAGSY equilibrium model, whose ideal-gas assumption, methane-centered kinetic set, and graphite-based char approximation limit the wide applicability of the predicted syngas yields when scaled beyond the laboratory. In addition, the environmental metrics that are reported here should be treated as indicative. Finally, minor sources of uncertainty, daily fluctuations in solar-still evaporation, small variations in feedstock composition, and the limited number of HTC batches, may shift mass and energy balances slightly, yet their impact is marginal and does not diminish the study’s central finding that the integrated HTC–solar distillation–co-gasification pathway is a technically promising route for the valorization of biomass pruning and sludge.

Further research will include the development of a full-scale Aspen Plus process model around a 25-kW biomass gasifier that is being installed in the Thermodynamic and Transport Phenomena laboratory of the National Technical University of Athens. This will allow rigorous heat-integration, separation, and utility analyses. These simulations will be coupled with cradle-to-gate carbon accounting to place the process on a verifiable net-emissions basis.

4. Conclusions

In this study, a sustainable energy proposal for Lesvos Island, leveraging the abundant local resource of olive pruning waste and addressing the challenge of sludge management was put forward. By considering the co-gasification of sludge and olive pruning,

- The process could significantly reduce landfilling costs while enhancing energy production.
- HTC is proposed as a method to convert sludge into HC, a carbon-rich product, without the need for drying sludge that typically contains 12% to 15% TS.
- Furthermore, the use of solar distillation as a low-energy method for drying the HTC effluent is particularly notable for its sustainability and resourcefulness in utilizing natural processes to reduce energy consumption.
- The combined approach of HTC, solar distillation, and gasification projected to increase total electricity production of Lesvos Island by 4720 MWh/year.
- This integrated solution not only promotes waste valorization but also contributes to the renewable energy production on the island. The text concludes with a call for

a thorough techno-economic analysis to fully understand the benefits and potential challenges of such an integrated system.

- This analysis would be crucial in evaluating the viability and economic attractiveness of the proposed system, as well as in identifying any technical or logistical obstacles that may need to be overcome for successful implementation.

Author Contributions: Conceptualization, S.V.; methodology, G.A. and D.L.; software, S.V. and D.L.; validation, G.A., D.L. and S.V.; formal analysis, A.A.; investigation, A.A.; resources, S.V.; data curation, A.A. and S.V.; writing—original draft preparation, G.A. and S.V.; writing—review and editing, D.L. and S.V.; visualization, S.V.; supervision, S.V.; project administration, S.V.; funding acquisition, S.V. All authors have read and agreed to the published version of the manuscript.

Funding: This research was funded by the European Union under the framework of HORIZON EUROPE with the grant agreement number 101181568 for the project BioFairNet.

Data Availability Statement: Data will be available on request.

Acknowledgments: During the preparation of this manuscript, the authors used ChatGPT 4.5 for the purpose of correcting linguistic errors. The authors have reviewed and edited the output and take full responsibility for the content of this publication.

Conflicts of Interest: The authors declare no conflicts of interest.

Abbreviations

The following abbreviations are used in this manuscript:

GHGs	Greenhouse Gasses
WWTPs	Wastewater Treatment Plants
S.S.	Sewage Sludge
AD	Anaerobic Digestion
A.D.S.	Anaerobically Digested Sludge
HTC	Hydrothermal Carbonization
HT	Hydrothermal Treatment
PTFE	Polytetrafluoroethylene
COD	Chemical Oxygen Demand
TS	Total Solids
VS	Volatile Solids
HHV	Higher Heating Value
MAGSY	Modelling of Advanced Gasification Systems
VCS	Villars–Cruise–Smith
OMWW	Olive Mill Wastewater
HC	Hydrochar
LHV	Lower Heating Value
MHV	Medium Heating Value

References

1. Wang, J.H.; Zhao, X.L.; Guo, Z.W.; Yan, P.; Gao, X.; Shen, Y.; Chen, Y.P. A full-view management method based on artificial neural networks for energy and material-savings in wastewater treatment plants. *Environ. Res.* **2022**, *211*, 113054. [[CrossRef](#)]
2. Shanmugam, K.; Gadhamshetty, V.; Tysklind, M.; Bhattacharyya, D.; Upadhyayula, V.K. A sustainable performance assessment framework for circular management of municipal wastewater treatment plants. *J. Clean. Prod.* **2022**, *339*, 130657. [[CrossRef](#)]
3. Ragi, K.B.; Ekka, B.; Mezule, L. Zero pollution protocol for the recovery of cellulose from municipal sewage sludge. *Bioresour. Technol. Rep.* **2022**, *20*, 101222. [[CrossRef](#)]
4. Xu, Z.; Jin, Q.; Wang, M.; Zhao, Y.; Wang, T.; Zhai, W.; Huang, Z.; Yang, G. Preparation of environmental remediation material based on manganese-slag and sewage sludge as a strategy for remediation of cadmium pollution. *J. Environ. Manag.* **2023**, *347*, 119096. [[CrossRef](#)]

5. Achkir, A.; Aouragh, A.; El Mahi, M.; Labjar, N.; Bouch, M.E.; Ouahidi, M.L.; Badza, T.; Farhane, H.; Moussaoui, T.E. Implication of sewage sludge increased application rates on soil fertility and heavy metals contamination risk. *Emerg. Contam.* **2023**, *9*, 100200. [[CrossRef](#)]
6. Urbaniak, M.; Baran, A.; Giebułtowicz, J.; Bednarek, A.; Serwecińska, L. The occurrence of heavy metals and antimicrobials in sewage sludge and their predicted risk to soil—Is there anything to fear? *Sci. Total Environ.* **2023**, *912*, 168856. [[CrossRef](#)] [[PubMed](#)]
7. Limmun, W.; Ishikawa, N.; Maeda, T.; Umeda, T.; Song, J.; Sasamoto, M.; Umita, T.; Ito, A. Exploration of an efficient method for removing antibiotics from water and digested sewage sludge using Fe (VI): Kinetics and P phytoavailability and compostability in treated sludge. *Chemosphere* **2023**, *336*, 139165. [[CrossRef](#)] [[PubMed](#)]
8. Merzari, F.; Goldfarb, J.; Andreottola, G.; Mimmo, T.; Volpe, M.; Fiori, L. Hydrothermal Carbonization as a Strategy for Sewage Sludge Management: Influence of Process Withdrawal Point on Hydrochar Properties. *Energies* **2020**, *13*, 2890. [[CrossRef](#)]
9. Tasca, A.L.; Puccini, M.; Gori, R.; Corsi, I.; Galletti, A.M.R.; Vitolo, S. Hydrothermal carbonization of sewage sludge: A critical analysis of process severity, hydrochar properties and environmental implications. *Waste Manag.* **2019**, *93*, 1–13. [[CrossRef](#)]
10. Xu, Z.X.; Ma, X.Q.; Zhou, J.; Duan, P.G.; Zhou, W.Y.; Ahmed, A.; Luque, R. The influence of key reactions during hydrothermal carbonization of sewage sludge on aqueous phase properties: A review. *J. Anal. Appl. Pyrolysis* **2022**, *167*, 105678. [[CrossRef](#)]
11. Malhotra, M.; Garg, A. Hydrothermal carbonization of centrifuged sewage sludge: Determination of resource recovery from liquid fraction and thermal behaviour of hydrochar. *Waste Manag.* **2020**, *117*, 114–123. [[CrossRef](#)]
12. Pérez, L.E.; Pérez, A.E.; Pino-Cortés, E.; Vallejo, F.; Díaz-Robles, L.A. An environmental assessment for municipal organic waste and sludge treated by hydrothermal carbonization. *Sci. Total Environ.* **2022**, *828*, 154474. [[CrossRef](#)]
13. Vakalis, S.; Georgiou, A.; Moustakas, K.; Fountoulakis, M. Assessing the effect of hydrothermal treatment on the volatile solids content and the biomethane potential of common reed (*Phragmites australis*). *Bioresour. Technol. Rep.* **2022**, *17*, 100923. [[CrossRef](#)]
14. Wang, L.; Chang, Y.; Li, A. Hydrothermal carbonization for energy-efficient processing of sewage sludge: A review. *Renew. Sustain. Energy Rev.* **2019**, *108*, 423–440. [[CrossRef](#)]
15. Maniscalco, M.P.; Volpe, M.; Messineo, A. Hydrothermal carbonization as a valuable tool for energy and environmental applications: A review. *Energies* **2020**, *13*, 4098. [[CrossRef](#)]
16. Rabea, K.; Michailos, S.; Akram, M.; Hughes, K.J.; Ingham, D.; Pourkashanian, M. An improved kinetic modelling of woody biomass gasification in a downdraft reactor based on the pyrolysis gas evolution. *Energy Convers. Manag.* **2022**, *258*, 115495. [[CrossRef](#)]
17. Nunes, L.J. Biomass gasification as an industrial process with effective proof-of-concept: A comprehensive review on technologies, processes and future developments. *Results Eng.* **2022**, *14*, 100408. [[CrossRef](#)]
18. Akbarian, A.; Andooz, A.; Kowsari, E.; Ramakrishna, S.; Asgari, S.; Cheshmeh, Z.A. Challenges and opportunities of lignocellulosic biomass gasification in the path of circular bioeconomy. *Bioresour. Technol.* **2022**, *362*, 127774. [[CrossRef](#)]
19. Srimalanon, A.; Kachapongkun, P. Synthesis gas production with gasification technology from municipal solid waste. *Appl. Sci. Eng. Prog.* **2023**, *16*, 6633. [[CrossRef](#)]
20. Situmorang, Y.A.; Zhao, Z.; Chaihad, N.; Wang, C.; Anniwaer, A.; Kasai, Y.; Abudula, A.; Guan, G. Steam gasification of co-pyrolysis chars from various types of biomass. *Int. J. Hydrogen Energy* **2021**, *46*, 3640–3650. [[CrossRef](#)]
21. Jeong, H.J.; Park, S.; Hwang, J. Co-gasification of coal–biomass blended char with CO₂ at temperatures of 900–1100 °C. *Fuel* **2014**, *116*, 465–470. [[CrossRef](#)]
22. Wei, J.; Guo, Q.; Gong, Y.; Ding, L.; Yu, G. Synergistic effect on co-gasification reactivity of biomass-petroleum coke blended char. *Bioresour. Technol.* **2017**, *234*, 33–39. [[CrossRef](#)] [[PubMed](#)]
23. Fona, Z.; Irvan, I.; Tambun, R.; Fatimah, F.; Setiawan, A.; Adriana, A. Review on advance catalyst for biomass gasification. *Appl. Sci. Eng. Prog.* **2024**, *17*, 7295. [[CrossRef](#)]
24. Lin, C.; Zuo, W.; Yuan, S.; Zhao, P.; Zhou, H. Effect of moisture on gasification of hydrochar derived from real-MSW. *Biomass Bioenergy* **2023**, *178*, 106976. [[CrossRef](#)]
25. Vasileiadou, M.A.; Altiparmaki, G.; Moustakas, K.; Vakalis, S. Quality of Hydrochar from Wine Sludge under Variable Conditions of Hydrothermal Carbonization: The Case of Lesvos Island. *Energies* **2022**, *15*, 3574. [[CrossRef](#)]
26. Mastoras, P.; Vakalis, S.; Fountoulakis, M.S.; Gatidou, G.; Katsianou, P.; Koulis, G.; Thomaidis, N.S.; Haralambopoulos, D.; Stasinakis, A.S. Evaluation of the performance of a pilot-scale solar still for olive mill wastewater treatment. *J. Clean. Prod.* **2022**, *365*, 132695. [[CrossRef](#)]
27. Leghari, A.; Laghari, A.A.; Kumar, A.; Rizwan, M.; Latif, A.; Kumari, L.; Laghari, M.; Ding, L.; Yu, G. Co-gasification of sewage sludge derived hydrochar and coal: Implications for syngas production and ash content. *Int. J. Hydrogen Energy* **2025**, *161*, 150682. [[CrossRef](#)]
28. APHA. *Standard Methods for the Examination of Water and Wastewater*, 20th ed.; American Public Health Association, Port City Press: Baltimore, MD, USA, 1998; p. 415.

29. Vakalis, S.; Moustakas, K. Applications of the 3T method and the R1 formula as efficiency assessment tools for comparing waste-to-energy and landfilling. *Energies* **2019**, *12*, 1066. [[CrossRef](#)]
30. Mendecka, B.; Lombardi, L.; Micali, F.; De Risi, A. Energy Recovery from Olive Pomace by Hydrothermal Carbonization on Hypothetical Industrial Scale: A LCA Perspective. *Waste Biomass Valorization* **2020**, *11*, 5503–5519. [[CrossRef](#)]
31. Patuzzi, F.; Prando, D.; Vakalis, S.; Rizzo, A.M.; Chiaramonti, D.; Tirler, W.; Mimmo, T.; Gasparella, A.; Baratieri, M. Small-scale biomass gasification CHP systems: Comparative performance assessment and monitoring experiences in South Tyrol (Italy). *Energy* **2016**, *112*, 285–293. [[CrossRef](#)]
32. Alipour, M.; Asadi, H.; Chen, C.; Rashti, M.R. Bioavailability and eco-toxicity of heavy metals in chars produced from municipal sewage sludge decreased during pyrolysis and hydrothermal carbonization. *Ecol. Eng.* **2021**, *162*, 106173. [[CrossRef](#)]
33. Petrovič, A.; Predikaka, T.C.; Vuković, J.P.; Jednačak, T.; Hribernik, S.; Vohl, S.; Urbanc, D.; Tišma, M.; Čuček, L. Sustainable hydrothermal co-carbonization of residues from the vegetable oil industry and sewage sludge: Hydrochar production and liquid fraction valorisation. *Energy* **2024**, *307*, 132760. [[CrossRef](#)]
34. Altıparmak, G.; Vasileiadou, M.A.; Vakalis, S. The effect of excess water on the hydrothermal carbonization of anise waste from ouzo production on Lesbos Island. *Sustain. Chem. Pharm.* **2022**, *29*, 100831. [[CrossRef](#)]
35. Kosińska, N.; Krzyżyńska, R.; Grosser, A.; Kwapińska, M.; Ghazal, H.; Jouhara, H.; Kwapiński, W. Hydrothermal carbonisation products energy properties: The role of digested sludge type and operating conditions. *Therm. Sci. Eng. Prog.* **2025**, *61*, 103461. [[CrossRef](#)]
36. Marin-Batista, J.D.; Mohedano, A.F.; Rodríguez, J.J.; De La Rubia, M.A. Energy and phosphorous recovery through hydrothermal carbonization of digested sewage sludge. *Waste Manag.* **2020**, *105*, 566–574. [[CrossRef](#)] [[PubMed](#)]
37. Oliveira, A.S.; Sarrión, A.; Baeza, J.A.; Diaz, E.; Calvo, L.; Mohedano, A.F.; Gilarranz, M.A. Integration of hydrothermal carbonization and aqueous phase reforming for energy recovery from sewage sludge. *Chem. Eng. J.* **2022**, *442*, 136301. [[CrossRef](#)]
38. Salimbeni, A.; Demey, H. Integrating hydrothermal carbonization and chemical leaching to recover biogenic carbon from sewage sludge. *J. Environ. Manag.* **2025**, *373*, 123516. [[CrossRef](#)]
39. Shrestha, A.; Acharya, B.; Farooque, A.A. Study of hydrochar and process water from hydrothermal carbonization of sea lettuce. *Renew. Energy* **2021**, *163*, 589–598. [[CrossRef](#)]
40. Selvaraj, P.S.; Ettiyagounder, P.; Sabarish, K.; Periasamy, K.; Rengasamy, B.; Veeraswamy, D.; Karchiyappan, T.; Kathirvel, S. Hydrothermal carbonization approach for transforming biomass waste to value added hydrochar and its applications in water remediation. *Desalination Water Treat.* **2025**, *322*, 101199. [[CrossRef](#)]
41. Duan, Z.; Li, C.; Zhang, Y.; Xu, D.; Zhi, Y.; Yakovlev, V.A.; Strizhak, P.A. Optimizing Co-hydrothermal carbonization of municipal sludge and enteromorpha prolifera for enhanced hydrochar yield and adsorption capacity using response surface methodology. *Algal Res.* **2025**, *90*, 104189. [[CrossRef](#)]
42. Zhi, Y.; Xu, D.; Jiang, G.; Yang, W.; Chen, Z.; Duan, P.; Zhang, J. A review of hydrothermal carbonization of municipal sludge: Process conditions, physicochemical properties, methods coupling, energy balances and life cycle analyses. *Fuel Process. Technol.* **2024**, *254*, 107943. [[CrossRef](#)]
43. Gong, M.; Liu, P.; Xu, F.; Xu, Q.; Feng, J.; Su, Y.; Fan, Y. A critical review on preparation, property prediction and application of sludge co-hydrothermal carbonization hydrochar as solid fuel. *J. Environ. Chem. Eng.* **2025**, *13*, 116458. [[CrossRef](#)]
44. Mazumder, T.S.; Mahmud, R.; Rahman, M.M.; Islam, M.S. Assessment of nutrient and heavy metal contents in a sewage sludge treatment plant through hydrothermal carbonization. *S. Afr. J. Chem. Eng.* **2025**, *53*, 117–126. [[CrossRef](#)]
45. Chen, D.; Qiu, P.; Liu, S.; Wang, W.; Sun, R.; Zhao, Y.; Zhang, L.; Liu, L.; Xing, C. Study on the combustion characteristics of micro-mixing nozzle unit at different syngas heating values. *Int. J. Hydrogen Energy* **2025**, *136*, 456–468. [[CrossRef](#)]
46. Saba, B.; Christy, A.D.; Shah, A. Hydrochar for pollution remediation: Effect of process parameters, adsorption modeling, life cycle assessment and techno-economic evaluation. *Resour. Conserv. Recycl.* **2024**, *202*, 107359. [[CrossRef](#)]

Disclaimer/Publisher's Note: The statements, opinions and data contained in all publications are solely those of the individual author(s) and contributor(s) and not of MDPI and/or the editor(s). MDPI and/or the editor(s) disclaim responsibility for any injury to people or property resulting from any ideas, methods, instructions or products referred to in the content.